

ADATIVE POWER CONTROL FACTOR AND EFFICIENCY OF FLYBACK CONVERTER FOR ACTIVE CLAMP SYSTEM

N MADHUKAR REDDY

Assistant Professor, Department of Electrical and Electronics Engineering, Siddhartha Institute of Technology and Sciences, Narapally, Hyderabad, Telangana, India

Abstract- This project presents an improvement of power factor and efficiency on fly back converter with Active Clamp Technique. The main objective of this project to suppress the harmonics and to improve power factor and efficiency. Flyback converter is widely adopted for low-power offline applications due to its simplicity and low cost. Usually, an RCD (Residual Current Devices) clamp technique is necessary to dissipate the leakage energy during the switch is OFF. In this method, the energy in the leakage inductance can be fully recycled. Soft switching can be achieved for the main switch and absorb the leakage energy is transferred to the output and input side. Compared to the conventional active clamp technique, the proposed methods can achieve high efficiency in light load condition, and the efficiency is not affected by leakage inductance. A Total harmonic distortion is reduced with this converter to increase efficiency. The simulation work of with and without Active clamp Flyback converter have been done using MATLAB/Simulink software

Key words: Active clamp method, Dc-Dc Converter, flyback converter, high efficiency, THD.

I. INTRODUCTION

A flyback converter due to minimum number of semiconductor and magnetic components, are widely adopted for offline low-cost power supplies. Another feature which makes it very attractive is its simplicity and low cost. The soft turn-on of the switch is highly desirable, as the voltage across the switch at the instant of turn-on is high. Soft switching is also useful as it minimizes the size and loss of the EMI filter. When the switch is OFF, an RCD clamp circuit is usually used to dissipate the leakage energy. In this paper a New active clamp technique is used to reduce THD as well as increase efficiency. The transformer used should be associated with minimized leakage inductance to reduce the voltage spikes across the switch, and hence achieve high efficiency.

The power supply designers still face the problem on how to further improve the

efficiency of the flyback converter [1] A solution to the problem of improving efficiency and reducing THD is reducing the leakage inductance energy loss. If the leakage inductance is large, the energy dissipated in the snubber resistor will be large, which in turn deteriorate the efficiency. The active clamp technology used on flyback converter will recycle the energy in the leakage inductor and can achieve soft – switching for the primary and auxillary switches. Hence, high efficiency can be achieved, but it is sensitive to parameters variations. Control schemes used to improve efficiency of the conventional flyback converter are mainly focussed on how to minimize the switching loss. The

conventional constant frequency control methodology on flyback converter has low efficiency due to high switching loss. This is

mainly caused by the high drain-to-source voltage across the switch. Hence, many variable frequency control schemes are developed to improve the performance compared to the conventional constant frequency control. The active clamp flyback converter can recycle the energy in the leakage inductor and achieve soft switching for both primary and auxiliary switch [2]–[8]. Although it has good performance in efficiency at full-load condition, it is sensitive to parameters variations. The variation of leakage inductance and snubber capacitor affects the conduction angle of the secondary-side rectifier, which lowers the efficiency. And the two active switches also increase the cost. Furthermore, the conventional complementary gate signal and constant frequency (CF) control method result in poor efficiency at light-load condition, which also leads to lower average efficiency. Also, many control schemes are proposed to improve the efficiency of the conventional flyback converter. They mainly focus on how to reduce the switching loss. In low-input voltage condition, zero voltage switching (ZVS) for primary-side switch can be achieved. And switching loss still exists in high-input condition. However, the switching frequency increases at light-load and high-input condition, which leads to a low-light-load efficiency. The maximum switching frequency need to be clamped to reduce the electromagnetic interference (EMI) noise and burst mode operation is necessary to improve the light-load efficiency [10]. In QR control, the ZVS of primary-side switch can be achieved if the secondary synchronous rectifier is adopted.

II. PRINCIPLE OF OPERATION

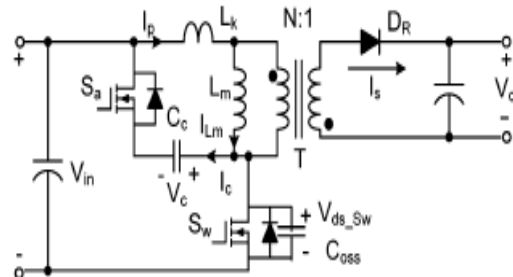


Fig. 1. Topology of the active clamp flyback converter.

Figure 1 shows the basic circuit diagram of a Flyback converter. Its main parts are the transformer, the primary switching MOSFET Q1, secondary rectifier D1, output capacitor C1 and the Pulse Generator. Depending on the design of T1, the Flyback can operate either in CCM (Continuous Conduction Mode) or DCM (Discontinuous Conduction Mode). In DCM, all the energy stored in the core is delivered to the secondary during the turn off phase (Flyback period), and the primary current falls back to zero before the Q1 switch turns on again. For CCM, the energy stored in the transformer is not completely transferred to the secondary; that is, the Flyback current (ILPK and ISEC) does not reach zero before the next switching cycle. Figure 2 & 3 shows the difference between DCM and DCM mode in terms of Flyback primary and secondary current waveforms [6].

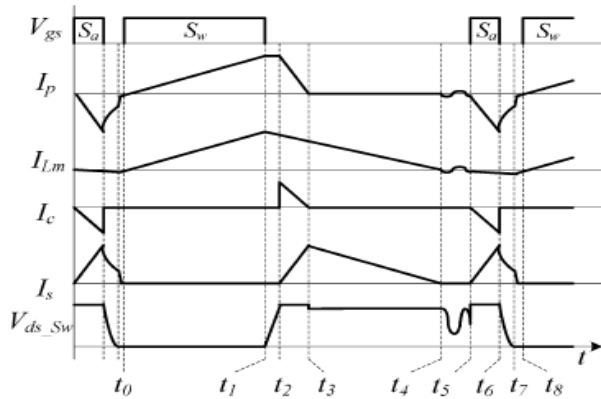


Fig. 2. Flyback Converter waveforms Under DCM operation

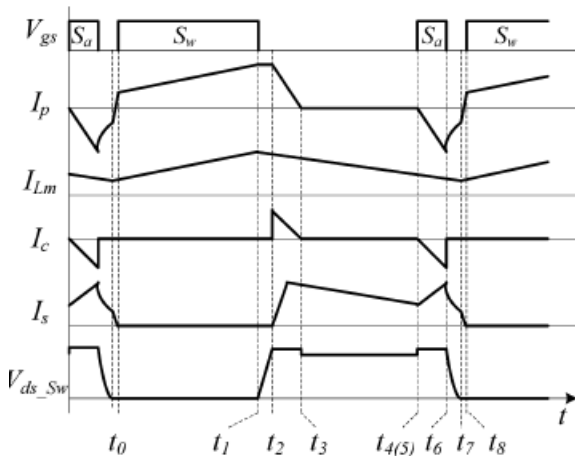


Fig. 3. Flyback Converter waveforms Under CCM operation

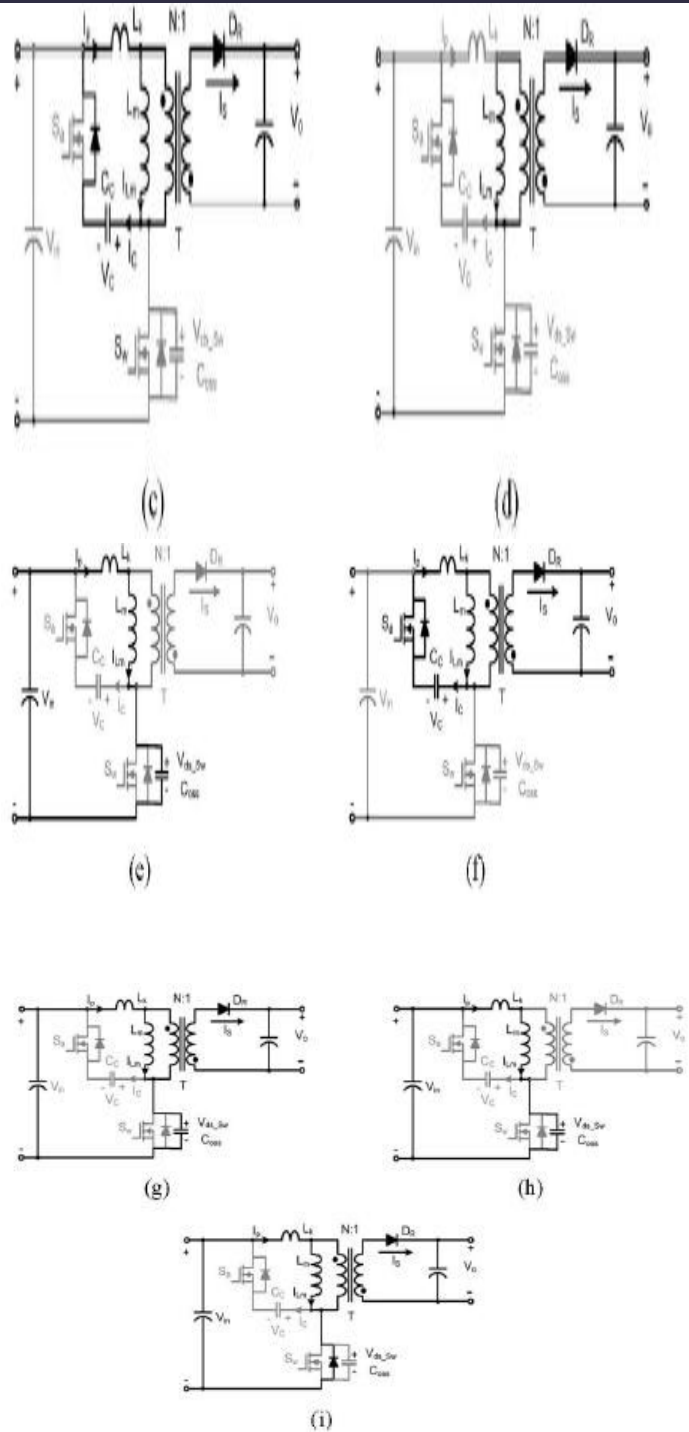


Fig. 4. Modes of Operation Flyback converter

(a) Mode 1 [$t_0 - t_1$].

(b) Mode 2 [$t_1 - t_2$]. (c) Mode 3 [$t_2 - t_3$]. (d)

Mode 4 [$t_3 - t_4$].

(e) Mode5 [$t_4 - t_5$]. (f) Mode 6 [$t_5 - t_6$]. (g)

Mode 7 [$t_6 - t_7$].

(h) Mode7B [$t_6 - t_7$].(i) Mode 8 [$t_7 - t_8$].

Mode 1 [$t_0 - t_1$]: In this mode, primary-side switch S_w is ON and the auxiliary switch S_a is OFF. The energy is stored to the magnetizing

inductor and the primary-side current I_p increases linearly, which is the same as the conventional flyback converter.

Mode 2 [t_1-t_2]: At t_1 , when S_w turns OFF, C_{oss} is charged up by the magnetizing current. Due to relative large magnetizing inductance, the drain-source voltage V_{ds} S_w of main switch S_w increases linearly.

Mode 3 [t_2-t_3]: At t_2 , the voltage V_{ds} S_w reaches $V_{in} + V_c$, the antiparalleled diode of S_a turns ON and the secondary-side rectifier D_R also turns ON. The energy stored in the magnetizing inductor starts to deliver to the output. And the energy in the leakage inductor is absorbed by the clamp capacitor. This mode can be treated as a primary to secondary commutation period.

Mode 4 [t_3-t_4]: At t_3 , the current through leakage inductance is zero and the antiparalleled diode of S_a is OFF. The magnetizing energy is delivered to the load as

conventional flyback converter and the magnetizing current decreases linearly.

Mode 5 [t_4-t_5]: At t_4 , magnetizing current decreased to zero, and D_R turns OFF. A parasitic resonance occurs between L_m and C_{oss} as conventional flyback at DCM condition.

Mode 6 [t_5-t_6]: At t_5 , auxiliary switch S_a is turned ON. The voltage across the magnetizing inductance L_m and leakage inductance L_k is clamped to V_c , and secondary winding is forward-biased, so D_R is ON. The current through L_k increases reversely.

Mode 7 [t_6-t_7]: At t_6 , the auxiliary switch S_a turns OFF. The negative current I_p discharges the parasitic capacitor C_{oss} . If the leakage energy is larger than the energy in the parasitic capacitor C_{oss} , the secondary D_R keeps ON, the difference between I_p and I_{Lm} is fed to the secondary side.

Mode 8 [t_7-t_8]: At t_7 , the output capacitor C_{oss} voltage decreased to zero and the antiparalleled diode of main switch S_w turns ON. If the leakage inductor current I_p is still larger than I_{Lm} , the equivalent circuit is shown in Fig. 4(i). If the leakage inductor current I_p reaches I_{Lm} during Mode 7, the equivalent circuit is same as Fig. 4(h). The primary-side switch S_w should be turned ON before the primary current I_p changes the polarity.

III. DESIGN CONSIDERATIONS

Based on the steady-state operation mode analysis discussed in Section II, there is an extra power deliver period when the auxiliary switch is ON. But the energy delivered to the load usually is quite small, which will not affect the output. The relationship of the key parameters of the clamp circuit will be discussed in this section, such as ZVS operation range, clamp capacitance, auxiliary switch ON time, and the clamp voltage. We still use DCM operation shown in Fig. 3 as an example. The conclusion can be adopted to

CCM directly [7]. Considering Non Ideal case let see the Design analysis based on modes of operation of converter. During Mode 3 and Mode 6, a simple equivalent circuit is given in Fig 6, an equivalent resistor R_{loss} is used to represent the circuit power loss [9]. Though the charge balance is still valid, the negative peak current I_{p-neg} is not equal to I_{pk} anymore, i.e., (1) is not valid any more. Also, the time T_a is not equal to T_{com} . The negative current can be given as follows:

$$i_p(t) = \frac{(V_{c0} - NV_o)}{L_k(s_2 - s_1)}(e^{s_1 t} - e^{s_2 t}) - \frac{I_{p0}}{(s_2 - s_1)}(s_1 e^{s_1 t} - s_2 e^{s_2 t}) \quad (1)$$

$$v_c(t) = \frac{V_{c0} - NV_o}{(s_2 - s_1)} (s_2 e^{s_1 t} - s_1 e^{s_2 t}) - \frac{I_{p0}}{C_c(s_2 - s_1)} (e^{s_1 t} - e^{s_2 t}) \quad (2)$$

$$s_1 = -\frac{R_{loss}}{2L_k} + \sqrt{\left(\frac{R_{loss}}{2L_k}\right)^2 - \frac{1}{L_k C_c}}$$

$$s_2 = -\frac{R_{loss}}{2L_k} - \sqrt{\left(\frac{R_{loss}}{2L_k}\right)^2 - \frac{1}{L_k C_c}} \quad (3)$$

where I_{p0} and V_{c0} are the initial current and voltage value at the beginning of the Mode 3 and Mode 6. During Mode 6, $I_{p0} = 0$ and $I_{p0} = I_{pk}$ during Mode 3. The clamp voltage should be estimated using charge balance during Mode 3 and Mode 6.

$$\begin{cases} T_{a-max} = \frac{\omega_d \pi}{2} \\ I_{p-neg-max} = \frac{(V_{c0} - NV_o)}{L_k \omega_d} e^{-bT_{a-max}} \end{cases} \text{ if } R_{loss} < 2\sqrt{\frac{L_k}{C_c}} \quad (4)$$

Where

$$\omega_d = \sqrt{(1/L_k C_c)^2 - b^2} \text{ and } b = R_{loss}/(2L_k).$$

To achieve soft switching of main switch, the negative peak current is much concerned. In the ideal condition, the I_{p-neg} always equals to I_{pk} as analyzed before. The extra damping effect caused by the circuit power loss reduces the negative peak value, which will affect the ZVS range.

IV. EXPERIMENTAL RESULTS

Table-1

Simulation Parameters

Parameter	Value
Input Voltage	230V

Output Voltage	25v
Output current	5A
Auxiliary switch ON Time	400ns
Transformer Turns Ratio	24:4:3
Magnetizing Inductance	260uH
Leakage Inductance	1.5uH
Clamp capacitor	220nF
Dead time	400ns

4.1 Simulation of flyback converter without active clamp technique.

The equivalent circuit loss resistance is dominated by the auxiliary switch ON resistance, i.e., around 5Ω . Based on the parameters given in Table I, the circuit is almost critical damping condition.

The Figure 5 & 6 shows the Simulation Diagram for flyback converter without clamping circuit and its Output voltage and current showed. The output voltage contains higher THD.

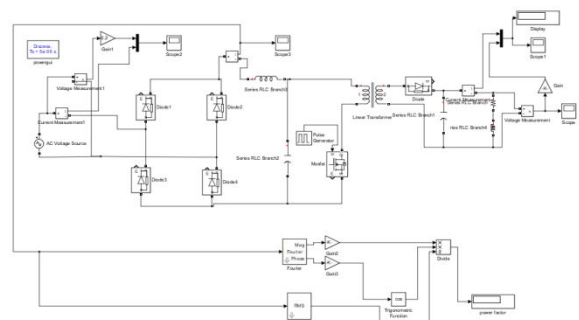


Fig.5 Simulation Diagram of flyback converter without active clamp technique

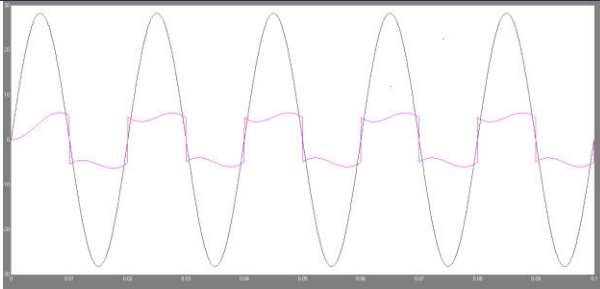


Fig.6 Input voltage and current waveforms of flyback converter without active clamp technique

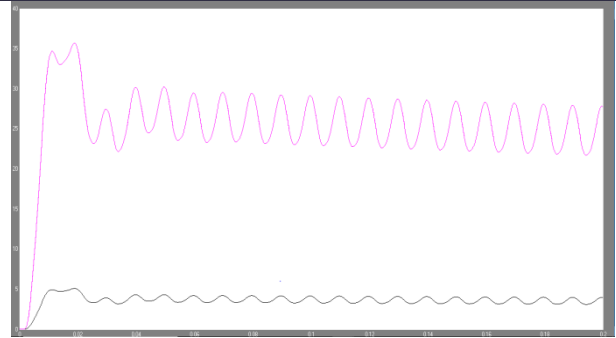


Fig.9 Output waveforms of flyback converter with new active clamp technique.

Figure 8 show simulation diagram of flyback converter with new active clamp technique. Figure 9 shows Output voltage and current across flyback converter with active clamping. The voltage is 27.6V and current is 5A. Figure 10 show THD plot with 12.76%.

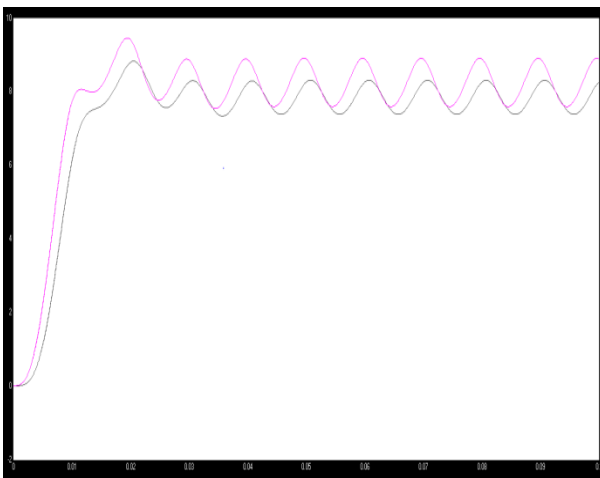


Fig.7 Output waveforms of flyback converter without active clamp technique

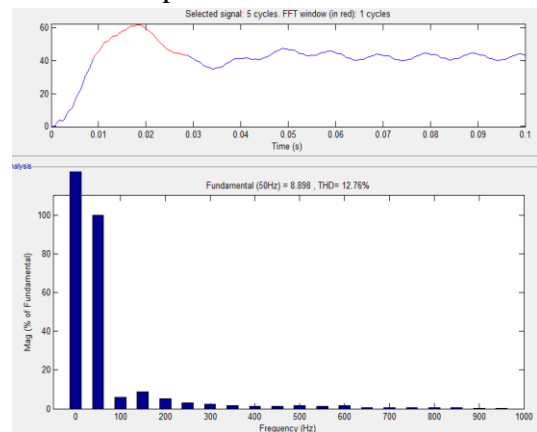


Fig.10 THD of flyback converter with new active clamp technique

4.2 Simulation of flyback converter with new active clamp technique.

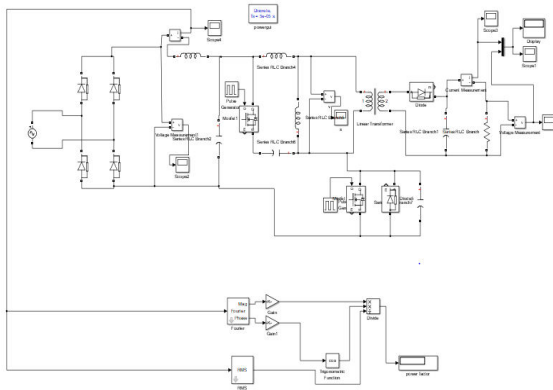


Fig.8 Simulation Diagram of flyback converter with new active clamp technique.

Table-2

Comparison between without active clamp and with active clamp

Parameter	Without Clamp	With Clamp
Input voltage	141.4	141.4
Power factor	0.82	0.96
Efficiency	77.8%	48%
THD	22.73%	12.76%

V. CONCLUSION

A Flyback converter with new active clamp technique with Soft switching operation is simulated. This converter satisfies the

requirement of low voltage and low power without the risk of extreme Duty ratios. The THD across this converter with clamp and without clamp is observed. This converter has high efficiency both for full load and light load condition, average efficiency also increases. High efficiency of flyback converter with new active clamp technique efficiency is 95% and THD is 12.76%.

References

- [1] T. Ninomiya, T. Tanaka, and K. Harada, "Analysis and optimization of a non dissipative LC turn-off snubber," *IEEE Trans. Power Electron.*, vol. 3, pp. 147–156, Apr. 1988.
- [2] C. T. Choi, C. K. Li, and S. K. Kok, "Control of an active clamp discontinuous conduction mode flyback converter," in *Proc. IEEE Power Electron. Drive Syst. Conf.*, 1999, vol. 2, pp. 1120–1123.
- [3] R. Watson, F. C. Lee, and G. Hua, "Utilization of an active-clamp circuit to achieve soft switching in flyback converters," *IEEE Trans. Power Electron.*, vol. 11, no. 1, pp. 162–169, 1992. (journal style)
- [4] Y.-K. Lo and J.-Y. Lin, "Active-clamping ZVS flyback converter employing two transformers," *IEEE Trans. Power Electron.*, vol. 22, no. 6, pp. 2416–2423, Nov. 2007.
- [5] B.-R. Lin, C.-C. Yang, and D. Wang, "Analysis, design and Implementation of an asymmetrical half-bridge converter," in *Proc. IEEE Int. Conf. Ind. Technol.*, 2005, pp. 1209–1214.
- [6] D. Fu, B. Lu, and F. C. Lee, "1 MHz high efficiency LLC resonant converters with synchronous rectifier," in *Proc. IEEE Power Electron. Spec. Conf.*, 2007, pp. 2404–2410.
- [7] D. Huang, D. Fu, and F. C. Lee, "High switching frequency high efficiency CLL resonant converter with synchronous rectifier," in *Proc. IEEE Energy Convers. Congr. Expo.*, 2009, pp. 804–809.
- [8] D. Fu, F. C. Lee, Y. Liu, and M. Xu, "Novel multi-element resonant converters for front-end dc/dc converters," in *Proc. IEEE Power Electron. Spec. Conf.*, 2008, pp. 250–256.
- [9] D. Fu, F. C. Lee, Y. Qiu, and F. Wang, "A novel high-power-density three-level LCC resonant converter with constant-power-factor-control for charging applications," *IEEE Trans. Power Electron.*, vol. 23, no. 5, pp. 2411–2420, Sep. 2008.
- [10] Y. Panov and M. M. Jovannovic, "Adaptive off-time control for variable frequency, soft-switched flyback converter at light loads," *IEEE Trans. Power Electron.*, vol. 17, no. 4, pp. 596–603, Jul. 2002.